Dual roles of zygotic and maternal Scribble1 in neural migration and convergent extension movements in zebrafish embryos

Hironori Wada[1], Miki Iwasaki[1,2], Tomomi Sato[1], Ichiro Masai[3], Yuko Nishiwaki[3], Hideomi Tanaka[1,2], Atsushi Sato[1,2,*], Yasuhiro Nojima[1,2] and Hitoshi Okamoto[1,2,†]

[1]Laboratory for Developmental Gene Regulation, Brain Science Institute, The Institute of Physical and Chemical Research (RIKEN), 2-1 Hirosawa, Wako, Saitama 351-0198, Japan
[2]Core Research for Evolutional Science and Technology (CREST), Japan Science and Technology Corporation (JST), 4-1-8 Honcho, Kawaguchi, Saitama 332-0012, Japan
[3]Masai Initiative Research Unit, RIKEN, 2-1 Hirosawa, Wako, Saitama 351-0198, Japan
*Present address: School of Bionics, Tokyo University of Technology, 1404 Katakura, Hachioji, Tokyo 192-0982, Japan
†Author for correspondence (e-mail: hitoshi@brain.riken.jp)

Accepted 2 March 2005

Development 132, 2273-2285
Published by The Company of Biologists 2005
doi:10.1242/dev.01810

Summary

In the developing vertebrate hindbrain, the characteristic trajectory of the facial (nVII) motor nerve is generated by caudal migration of the nVII motor neurons. The nVII motor neurons originate in rhombomere (r) 4, and migrate caudally into r6 to form the facial motor nucleus. In this study, using a transgenic zebrafish line that expresses green fluorescent protein (GFP) in the cranial motor neurons, we isolated two novel mutants, designated *landlocked* (*llk*) and *off-road* (*ord*), which both show highly specific defects in the caudal migration of the nVII motor neurons. We show that the *landlocked* locus contains the gene *scribble1* (*scrb1*), and that its zygotic expression is required for migration of the nVII motor neurons mainly in a non cell-autonomous manner. Taking advantage of the viability of the *llk* mutant embryos, we found that maternal expression of *scrb1* is required for convergent extension (CE) movements during gastrulation. Furthermore, we show a genetic interaction between *scrb1* and *trilobite(tri)/strabismus(stbm)* in CE. The dual roles of the *scrb1* gene in both neuronal migration and CE provide a novel insight into the underlying mechanisms of cell movement in vertebrate development.

Key words: Zebrafish, *landlocked*, *scribble1*, facial motor neuron, neuronal migration, convergent extension

Introduction

Among the mammalian cranial nerves, the facial (nVII) motor nerve shows a very characteristic trajectory within the hindbrain. The axons first project medially and anteriorly, and then make a turn around the abducent (nVI) nucleus. This projection is generated by caudal migration of the nVII motor neurons during embryonic development. This developmental process is also conserved in zebrafish (Higashijima et al., 2000; Bingham et al., 2002) (summarized in Fig. 1). The first-born nVII motor neurons appear in rhombomere (r) 4 at 16 hours post-fertilization (hpf) at the ventral surface of the hindbrain near the floor plate, followed by continuous production of the neurons up to 36 hpf. Soon after their birth, the nVII motor neurons start migrating caudally into r5, resulting in a row of the migrating neurons in the ventral hindbrain. At the same time, the migrating neurons extend axons anteriorly then laterally to exit the hindbrain at r4. These peripheral axons project to the branchial arches and anterior/posterior lateral lines. In 24 hpf, the first-born nVII motor neurons reach r6, where they turn laterally to form the facial nucleus. The later-born neurons follow the same pathway in serial order. After 48 hpf, most of the nVII motor neurons are localized in the r6 region.

Several mechanisms have been implicated in the caudal migration of r4-derived nVII motor neurons. In *hoxb1* knockout mice, r4-derived nVII motor neurons fail to migrate caudally (Studer et al., 1996). In chick hindbrain, they fail to migrate caudally and form a nucleus at r4. However, replacement of r5 or r6 with that of mouse restored caudal migration of the nVII motor neurons in chick hindbrain, indicating that in mice, r5 or r6 may emanate guidance cues to which chick nVII motor neurons can respond (Studer, 2001). Other molecules that regulate this migration have been recently and unexpectedly identified in zebrafish in studies on the convergent extension (CE) movements during gastrulation. The *trilobite/stbm* (*tri/stbm*) and *prickle1* (*pk1*) gene products were shown to regulate both CE and migration of the nVII motor neurons (Bingham et al., 2002; Jessen et al., 2002; Carreira-Barbosa et al., 2003). In *Drosophila*, both Stbm and Prickle are involved in planar cell polarity (PCP) in epithelial cells in a Frizzled (Fz)/Dishevelled (Dsh)-dependent manner, and this pathway is referred to as the PCP pathway (reviewed by Strutt, 2003). These suggest that CE and neuronal migration may share common mechanisms that are associated with the PCP pathway.

However, in zebrafish, there is evidence that CE may also be regulated by other PCP signaling molecules encoded by *knypek(kny)/glypican4/6*, *silberblick(slb)/wnt11* and *pipetail(ppt)/wnt5a* (Topczewski et al., 2001; Heisenberg et al., 2000; Kilian et al., 2003), but disruption of these genes does

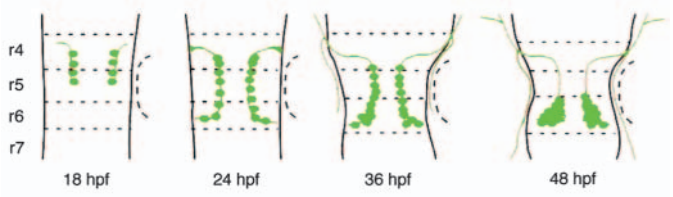

Fig. 1. Schematic drawing of migration of the nVII motor neurons in zebrafish. Dorsal views of the zebrafish hindbrain at each developmental stage. The nVII motor neurons and their axons are shown in green. Broken lines indicate rhombomeric boundaries. See text for details.

not impair migration of the nVII motor neurons (Bingham et al., 2002; Jessen et al., 2002), suggesting that the genetic cascades underlying neuronal migration and CE are not identical. In this study, we attempted to isolate novel mutants that were deficient in neuronal migration but retained normal CE movements. Such mutants would enable us to address the question of how the migration of the nVII motor neurons is related to the differentiation and function of these neurons.

In a systematic screen using the zebrafish transgenic Isl1-GFP strain, which expresses green fluorescent protein (GFP) in the branchiomotor neurons (Higashijima et al., 2000), we identified two novel mutants, denoted *landlocked* (*llk*) and *off-road* (*ord*), which displayed specific impairment of migration of the nVII motor neurons without any disruption of CE movements. The *llk* locus encompasses *scribble1* (*scrb1*), a homologue of the *Drosophila* cell polarity gene *scribble*. Here, we show that the zygotic expression of the *llk/scrb1* gene is required for migration of the nVII motor neurons mainly in a non cell-autonomous manner. In zygotic *llk* embryos, migration of the VII motor neurons is specifically impaired without any effect on CE movements. The zygotic *llk* embryos are homozygously viable, which meant we could obtain embryos deficient for both the maternal and zygotic contribution of *llk* transcripts. Depletion of maternal expression of *llk/scrb1* impaired CE movements. Furthermore, we show that proper interaction of Llk/Scrb1 with Tri/Stbm plays a crucial role in the regulation of CE movements.

Materials and methods

Fish strains and mutagenesis

Zebrafish (*Danio rerio*) were maintained according to standard procedures (Westerfield, 1995). The Isl1-GFP line (Higashijima et al., 2000) was derived from the RIKEN wild-type strain. The WIK strain was used for the genetic mapping (Shimoda et al., 1999). Mutagenesis was carried out as described previously (Masai et al., 2003; Solnica-Krezel et al., 1994). Mutations were induced in the male germ cells of the Isl1-GFP fish using *N*-ethyl-*N*-nitrosourea (ENU, Sigma). To isolate mutants deficient in migration of the VII neurons, embryos from the F_2 pairwise crosses were observed at 2 days post-fertilization (dpf) under a fluorescent dissecting microscope (Leica MZFLIII). Digital images were captured using a CCD camera (Hamamatsu C5810). A total of 1816 haploid genomes (1171 families) were screened (see supplementary material). Two alleles for the *llk* locus ($llk^{rw16}$and llk^{rw468}), four alleles for the *ord* locus (ord^{rw71}, ord^{rw135}, ord^{rw166}, ord^{rw380}) and one allele for the *tri* locus (tri^{rw75}) were identified. Images were captured using a fluorescence dissecting microscope (Leica MZFLIII) with a CCD camera (Hamamatsu C5810).

Immunohistochemistry and in situ hybridization

Standard protocols were used for immunohistochemistry with a zn-5 antibody (Oregon Monoclonal Bank, 1:100 dilution) (Trevarrow et al., 1990), anti-acetylated α-tubulin antibody (Sigma, 1:1000) and a secondary antibody conjugated to Alexa Fluor 533 (Santa Cruz Biotechnology, 1:500). The samples were viewed by confocal microscopy (Zeiss LSM 510). In situ hybridization using RNA probes was carried out as described previously (Westerfield, 1995). Digital images of the embryos were captured using a differential interference contrast (DIC) microscope (Zeiss Axioplan2) with a CCD camera (Olympus DP50). In each experiment involving comparison between wild-type and mutant embryos, we used embryos obtained from heterozygous parents and identified mutant homozygous embryos by observing expression of GFP. At least 20 embryos were stained and observed in each experiment.

Restrograde labeling and cell transplantation

Retrograde labeling of reticulospinal neurons with rhodamine-conjugated dextran (Molecular Probes) was carried out as described previously (Moens et al., 1996). Retrograde labeling of putative octavolateralis efferent (OLe) neurons with DiI (Molecular Probes) was also performed as described previously (Higashijima et al., 2000). The putative OLe neurons extend axons to the anterior and posterior lateral lines. The OLe axons exit the hindbrain at the r4 and r6 level at 24 hours post-fertilization (hpf) and extend anteriorly or posteriorly at 28 hpf (Higashijima et al., 2000). The DiI was applied, at 30 hpf, to the anterior or posterior lateral line ganglion regions, through which the OLe axons extend. Co-localization of DiI and GFP signals in the cell bodies was confirmed in each optical section of confocal microscopy (see Fig. S1 in supplementary material). From a total of 20 embryos, six wild-type embryos (three anterior and three posterior lateral line ganglia) and six llk^{rw16} homozygous embryos (four anterior and two posterior lateral line ganglia) were successfully labeled.

Cell transplantation was carried out according to standard protocols (Westerfield, 1995). llk^{rw16} homozygous embryos were produced by crossing llk^{rw16} homozygous parents. Cells from dome-stage (4-5 hpf) donor embryos injected with rhodamine-conjugated dextran were transplanted into shield-stage (6 hpf) host embryos as described previously (Moens et al., 1996). Mosaic embryos were analyzed alive at 36 hpf. To ensure that the transplanted donor cells were nVII motor neurons, we observed peripheral axons from donor cells labeled with rhodamine. In all of the mosaic embryos examined (three wild type>mutant and two mutant>wild type), a part of the facial motor axons bundle was rhodamine labeled, confirming that these donor cells were nVII motor neurons.

Mapping the mutant locus

In total, 1027 *llk* homozygous embryos (2054 meioses) were collected from parents derived from a llk^{rw16} homozygous fish × WIK cross. Genomic DNA was extracted from individual embryos at 3 dpf. PCR analysis with SSLP markers (Shimoda et al., 1999) was carried out to assign the *llk* locus to the linkage group. Representational differential analysis (RDA) was carried out as described previously (Lisitsyn et al., 1993; Sato and Mishina, 2003; Matsuda and Mishina, 2004). Genomic DNA was extracted from pools of 20 homozygous mutant fish and five wild-type siblings at 30 dpf. Amplicons were prepared by digesting pooled mutant genomic DNA (4 μg) and pooled wild-type genomic DNA (4 μg) with *Xba*I, *Eco*RI, *Bam*HI, *Spe*I and *Nco*I. The interactive hybridization-amplification step was repeated three times. The resulting RDA products were cloned and their flanking genomic sequences were obtained from the Sanger Centre genome database. Specific primers were designed, and PCR products amplified from the DNA of each mutant embryo of the mapping F_2 panel were digested with the appropriate enzymes to detect restriction enzyme length polymorphisms. Four RDA products (*Nco*I-10, *Xba*I-1, *Xba*I-4, and *Eco*RI-46) were successfully mapped near the *llk* locus (see text). The following primers and enzymes were used:

*Nco*I-10: amplified with 5′CAGGGAGGGAAGCTTAGGTTTT3′ and 5′GTCAGGACCTTGGTTTAAGGTC3′, digested with *Msp*I.

*Xba*I-1: amplified with 5′GAGGACATCCGCTGGTTACAA3′ and 5′CTGTACTTGTGTCCTGCAGT3′, digested with *Hae*III.

*Xba*I-4: amplified with 5′TGGTTGTAACCAGTGCTTGAC3′ and 5′ACCCTTCCAAACTCACACGC3′, digested with *Dra*I.

*Eco*RI-46: amplified with 5′TGAAACAAGTCCTAAAGGTCTTG3′ and 5′CATCAAGCAGGAGTGCTATC3′, digested with *Eco*RI.

Identification of the gene

A zebrafish PAC library (BUSUMP, RZPD) was screened by PCR using standard procedures. Specific primers from the EcoRI-46 flanking genome sequence were used for the amplification step (5′TTAAGGCAGAACAGGGAAGTGAGATCAAC3′ and 5′ACCTGTGATGTAGAGAGTCACC3′). Both ends of the resulting PAC were sequenced, and consistency with the database was confirmed. The *scrb1* genomic region was covered by a PAC clone (BUSUM#149G1) and the database contigs (AL772146 and z06s003613). To isolate the *scrb1* gene, total RNA was extracted from 24-hpf llk^{rw16} and llk^{rw468} homozygous embryos using an RNA extraction kit (Nippon gene). *scrb1* cDNA was amplified with a first strand cDNA synthesis kit (Takara) and PCR using specific primers designed from the database genomic sequences. The amino acid sequence of *llk/scrb1* was deduced from the nucleotide sequences of nine partial cDNAs. To exclude nucleotide changes derived from polymorphisms, genomic DNA from male grandparents of the family containing the llk^{rw16} and llk^{rw468} mutations was also sequenced. Six alternatively used exons 16, 28, 31, 34, 40 and 43 (see text in detail) were identified and RT-PCR analyses were performed to show the predominant *scrb1* product. Total RNAs extracted from 1.5, 10, 18, 24, 36 and 48-hpf embryos were used. Specific primers designed in the flanking regions of each exon are as follows:

exon 16: 5′CTAGATGCAGCAGAGCTAGA3′ and 5′AATACCCTCATCGTCACCT3′,

exon 28: 5′GTCGACAGAGACCTGAGTCC3′ and 5′AGTTTCCTCCTCCAGCAA3′,

exon 31: 5′GCTTCACCATCTGAGCCTTTC3′ and 5′TTGGACTACTGTGGCCATC3′,

exon 34: 5′ACTAAACCTGGTGCCATCCA3′ and 5′TGTTCTGGACTGTGCCTAC3′,

exon 40: 5′TTGGACAAGGAGCTGTCGCCTGC3′ and 5′CCATTGGTGTTGGAGAGGGTG3′,

exon 43: 5′CCACACCCTCTCCAACACCAAT3′ and 5′CTGCGTTACTGGAGGACTC3′.

For in situ hybridization, we used a partial cDNA fragment from the N-terminal region of the *scrb1* gene (157-418 aa, corresponding to the LRR domain), which detects all of the spliced variants. The primers used to isolate the cDNA fragments were as follows: 5′GAATCTACTGAAATCCTTGCC3′ and 5′GTTGGGGCAGCAGGTAGCAGG 3′.

The PCR products were cloned into the TA cloning vector, pCRII-TOPO (Invitrogen), and sequenced using a BigDye terminator cycle sequencing kit (PE Applied Biosystems) with an automated DNA sequencer (ABI PRISM/3100 Genetic Analyzer).

The accession number of *scrb1* is AB188388.

mRNA injection and detection of protein localization

The *scrb1* gene and mutated variants ($scrb1^{rw16}$, $scrb1^{rw468}$) were amplified by RT-PCR. To make the $scrb1^{\Delta PDZs}$ construct, the N-terminal 423-amino acid region of the *scrb1* gene was amplified by RT-PCR. The *stbm* gene was amplified by RT-PCR as previously described (Jessen et al., 2002). All of these genes were subcloned into pCS2 expression vectors and verified by sequencing. Sense-capped mRNA was synthesized using mMessage mMachine (Ambion) according to the manufacturer's guidelines. Approximately 1 nl of mRNA was injected into one-cell stage embryos at a concentration of 0.5 mg/ml in Danieau buffer (0.5 ng per embryo). To observe subcellular localization of the expressed proteins, GFP-fused genes (Scrb:GFP, $Scrb1^{rw16}$:GFP, $Scrb1^{\Delta PDZs}$:GFP and GFP:$Scrb1^{rw468}$) were generated and mRNA was injected as described. Five samples injected with each construct were observed by confocal microscopy at 10-12 hpf.

Knockdown by anti-sense morpholino oligonucleotides

Antisense morpholino oligonucleotides (MO) were designed by Gene Tools to target the *llk/scrb1* gene:

MO/ATG: 5′CCACAGCGGGATACACTTCAGCATG3′

MO/2e2i: 5′ACAAAAGTTTGCATACCATTTCTAG3′

Corresponding control MOs were as follows (lower case letters indicate mispaired residues):

MO/ATG-5mis: 5′CCAaAGaGGGATAaACTTGAGaATG3′

MO/2e2i-5mis: 5′AgAAAAcTTTcCATACgATTTgTAG3′

The MO/ATG was designed for targeting the putative AUG translation start site (underlined) and the MO/2e2i was designed for targeting the boundary of the second exon and the second intron (underlined) according to the manufacturer's instructions. The MO to the *tri/stbm* was designed as previously described (Jessen et al., 2002). Approximately 1 nl of MO was injected into one-cell stage embryos at concentrations of 5 or 0.5 mg/ml in Danieau buffer (5 or 0.5 ng per embryo) as described (Nasevicius and Ekker, 2000).

Labeling and tracing the r4-derived cell movements

Caged fluorescein-conjugated dextran (Molecular Probes) was injected into 1-cell stage Isl1-GFP embryos, and then the whole r4 region was exposed to UV illumination at 16 hpf using a fixed-stage microscope (Olympus BX-51WI) modified with special optics for uncaging experiments as previously described (Ando et al., 2001; Ando et al., 2003; Kozlowski and Weinberg, 2000). Three embryos were fixed at 24 hpf, and subjected to antibody staining using an anti-fluorescein antibody (Molecular Probes), anti-GFP antibody (Santa Cruz Biotechnology, 1:500), and secondary antibodies conjugated to Alexa Fluor 488 and 533.

Results

landlocked and *off-road* are novel mutants with disrupted migration of the nVII motor neurons

The Isl1-GFP transgenic line expresses GFP in the branchial motor neurons of the hindbrain (Higashijima et al., 2000). Using this line, we screened a total of 1816 haploid genomes mutagenized with *N*-ethyl-*N*-nitrosourea (ENU). Two novel mutants that showed perturbed migration of the r4-derived nVII motor neurons compared to wild-type were isolated. These were designated *landlocked* (*llk*; Fig. 2B,F,J, compare with the wild-type embryos shown in A,E,I) and *off-road* (*ord*; Fig. 2C,G,K). We also identified a novel allele for the *trilobite* (*tri*) mutant (Fig. 2D,H,L), in which CE movements were also impaired (Fig. 2D; Bingham et al., 2002; Jessen et al., 2002). Subsequent experiments further characterized the *llk* mutation.

Migration, but not differentiation, of the nVII motor neurons is impaired in the *llk* embryos

In wild-type embryos, the nVII motor neurons originated and began to express GFP in r4 at 16 hpf, after which they started to migrate caudally through r5 into r6 (Fig. 3A,C) (Chandrasekhar et al., 1997; Higashijima et al., 2000). The nVII motor neurons form the facial motor nucleus exclusively in r6 at 2 dpf (Fig. 3E). We examined two alleles of *llk* (llk^{rw16} and llk^{rw468}) that caused equivalent disruption of migration of the GFP-positive cells. All of the homozygous embryos (*n*=211

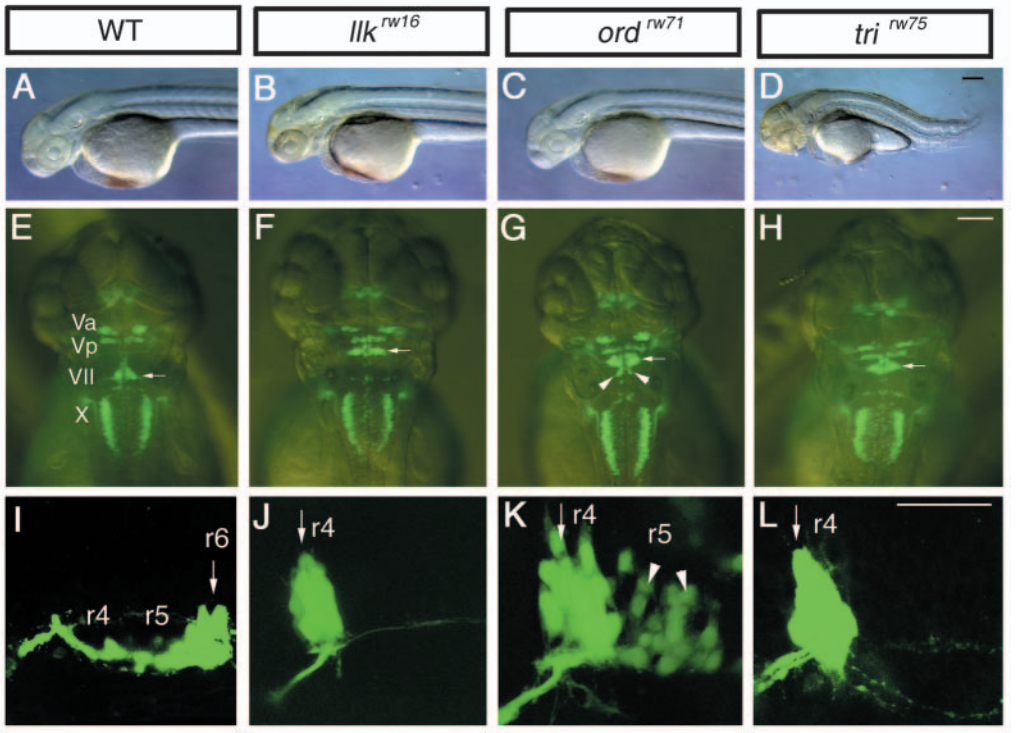

Fig. 2. Isolation of mutants with disrupted migration of the nVII motor neurons. Morphology and Isl1-GFP expression in the wild-type (A,E,I), *llk*^{rw16} (B,F,J), *ord*^{rw71} (C,G,K), and *tri*^{rw75} homozygous embryos (D,H,L) at 2 dpf (A-H) and 30 hpf (I-L). In the wild-type embryos, the nVII motor neurons are located in r6 (E,I, arrows). In contrast, in the *llk*^{rw16} and *tri*^{rw75} embryos the nVII motor neurons are located in r4 (F,J,H,L, arrows). In the *ord*^{rw71} embryos, the nVII motor neurons are located in r4 and r5 (G,K, arrowheads indicate cells migrating into r5). The cells that migrated into r5 became detached from the surface of hindbrain, and were scattered inside the hindbrain. The *tri*^{rw75} embryos show severe defects in the extension of the trunk region (D). The *llk* and *ord* embryos did not show any morphological abnormalities, in contrast to the *tri* embryos (B,C). (A-D, I-L) Lateral views; anterior is to the left, (E-H) dorsal views; anterior is to the top. Scale bars: 50 μm.

for *llk*^{rw16} and *n*=121 for *llk*^{rw468}) showed complete loss of migration of r4-derived GFP-expressing cells (Fig. 3B,D,F).

Although r6-derived GFP-expressing neurons (putatively octavolateralis efferent (OLe) neurons) also failed to migrate to r7 in the *llk* embryos (Fig. 3M-P, see also Fig. S1 in supplementary material), all the other migratory cell types were unaffected. The mutant embryos had normal tangential and radial migration of the trigeminal (nV) and vagus (nX) motor neurons (Fig. 2F), migration and positioning of the pigment cells derived from the neural crest (data not shown), and migration of lateral line neuromast cells derived from placode cells (data not shown). Thus, we concluded that the *llk* embryos had specific impairment of migration of the nVII motor neurons.

Tag-1 is a specific marker for migrating nVII motor neurons (Fig. 3G) (Warren et al., 1999). The non-migratory cells in the *llk* embryos still expressed *tag-1* mRNA (Fig. 3H), suggesting that these cells retained the potential to differentiate normally into nVII motor neurons. Consistent with this, these non-migratory cells extended the GFP-positive peripheral axons normally (Fig. 3I,J). The axons in the *llk* embryos projected to the correct specific target muscles with the same pattern as observed in wild-type embryos (Fig. 3K,L).

Patterning of the hindbrain is unaffected in the *llk* embryos

Each rhombomere shows differential expression of several genes which are essential for the fate determination of that specific rhombomere. *hoxb1a*, *krox20* and *valentino(val)/mafB* are expressed in r4, r3/5 and r5/6, respectively, in the developing zebrafish hindbrain (Prince et al., 1998; Oxtoby and Jowett, 1993; Moens et al., 1998). The patterns of expression of *hoxb1a* (Fig. 4A,B), *krox20* (Fig. 4C,D) and *val/mafB* (Fig. 4E,F) were identical between the *llk* and wild-type embryos, suggesting that the segmental patterning of the rhombomeres was normal in the mutant embryos.

The zn-5 antibody specifically labels segmentally repeated commissural axons in the zebrafish hindbrain (Trevarrow et al., 1990). The formation of zn-5-immunoreactive axons appeared normal in the *llk* embryos (Fig. 4G,H). Furthermore, labeling of the reticulospinal neurons by injecting a tracer dye into the spinal cord (Metcalfe et al., 1986; Moens et al., 1996) revealed that the anterior-posterior patterning of the reticulospinal neurons in the *llk* embryos was identical to that in the wild-type embryos (Fig. 4I,J). Together, these results suggest that the overall patterning and differentiation of the hindbrain neurons were unaffected by the *llk* mutation.

llk encodes zebrafish *scribble1*

The *llk* locus was genetically mapped to linkage group 7 between the SSLP markers, Z11545 and Z62080 (Shimoda et al., 1999) (Fig. 5A). To isolate DNA fragments closely associated with the *llk* locus, a representational differential analysis (RDA) (Lisitsyn et al., 1993; Sato and Mishina, 2003; Matsuda and Mishina, 2004) was performed. Four RDA products were closely linked to the *llk* locus and one of them, EcoRI-46, showed no recombination per 2054 meioses in F_2 crosses (Fig. 5A). The DNA fragments carrying the EcoRI-46 sequence were obtained by screening a PAC library together with a search of the Sanger Center genome database. The EcoRI-46 site was located in the first intron of a gene (Fig. 5B) that is highly homologous to mouse *Scrb* (Fig. 5F) (Murdoch et al., 2003). Sequence analyses of cDNA revealed that at least exons 16, 28, 31, 34, 40 and 43 were differentially used by alternative splicing (Fig. 5C). Two of them (exons 16 and 43) corresponded to those used in mouse *Scrb* [exons 16 and 36 in mouse (Murdoch et al., 2003)]. RT-PCR was performed and the most predominant transcript that putatively encoded a 1724

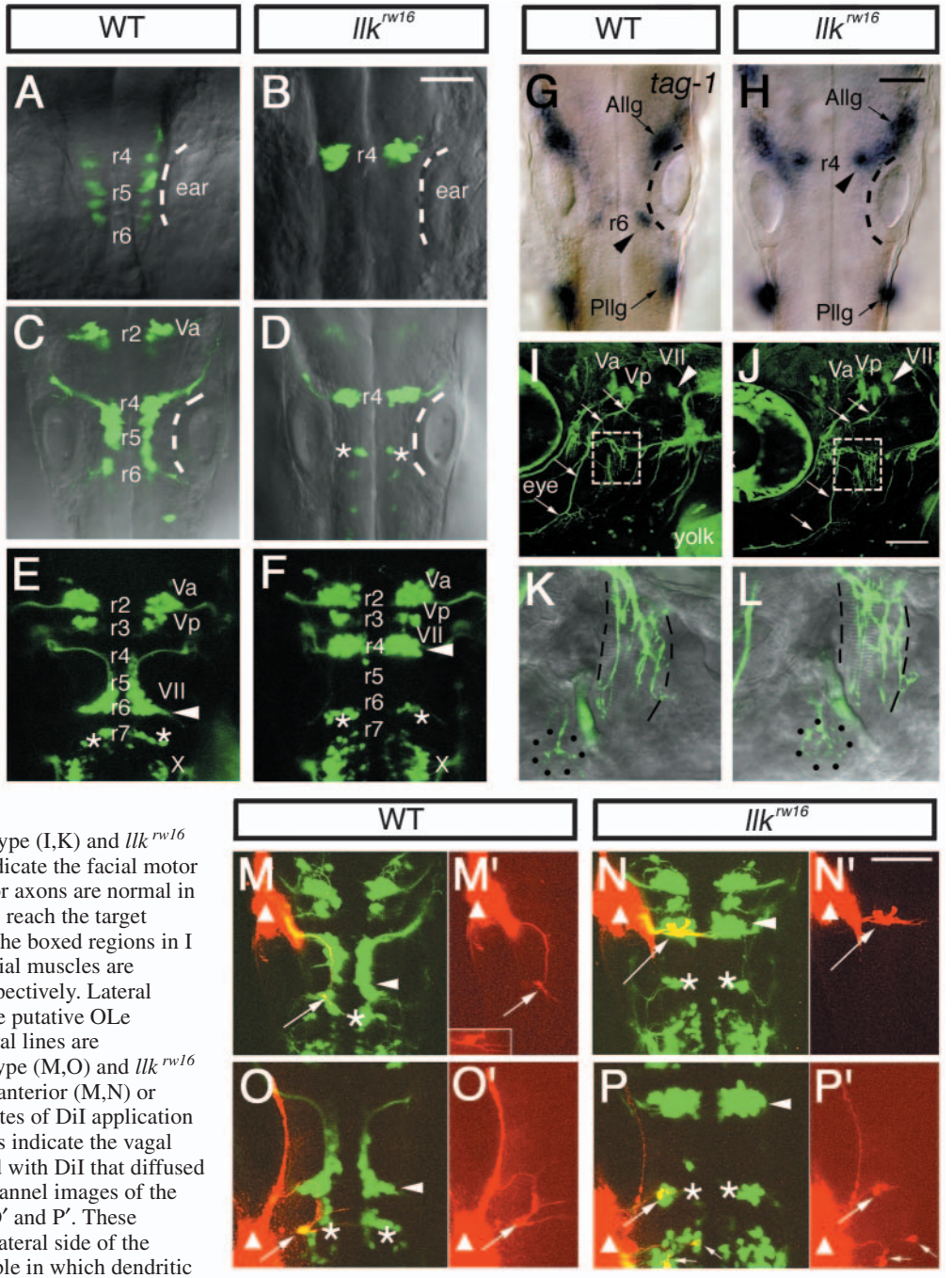

Fig. 3. Migration of the nVII motor neurons is specifically impaired in *llk* embryos. A-F, Isl1-GFP expression in the wild-type (A,C,E) and *llk*^{rw16} homozygous embryos (B,D,F) at 18 hpf (A,B), 24 hpf (C,D), and 48 hpf (E,F). In the wild-type siblings, the nVII motor neurons arise in r4, migrate caudally through r5 into r6 and form the nucleus in r6 (E, arrowhead). In contrast, in the *llk*^{rw16} embryos the GFP-expressing cells that arise in r4 fail to migrate and form an ectopic nucleus in r4 (F, arrowhead). Asterisks (D,E,F) indicate r6-derived putative OLe neurons, which migrate into r7 in the wild-type embryos. These neurons also fail to migrate in the mutant embryos and remain in r6 (D,F). (G,H) *tag-1* mRNA expression in the wild-type (G) and *llk*^{rw16} (H) embryos at 24 hpf. *tag-1*-positive cells are located in r4 in the *llk*^{rw16} embryo (H, arrowhead). Dorsal views. The position of the ears are indicated by the broken lines. Va, Vp, anterior and posterior trigeminal nuclei, respectively; VII, facial nucleus; X, vagus nucleus; Allg, Pllg, anterior and posterior lateral line ganglion, respectively. (I-L) Isl1-GFP expression in the wild-type (I,K) and *llk*^{rw16} (J,L) embryos at 5 dpf. Arrowheads indicate the facial motor nucleus. The trajectories of facial motor axons are normal in the *llk*^{rw16} embryo (arrows). The axons reach the target organs (K,L, higher magnifications of the boxed regions in I and J). Lateral line organs and the cranial muscles are indicated by dots and broken lines, respectively. Lateral views; anterior is to the left. (M-N) The putative OLe neurons (arrows) projecting to the lateral lines are retrogradely labeled (red) in the wild-type (M,O) and *llk*^{rw16} (N,P) embryos. DiI was applied to the anterior (M,N) or posterior lateral line ganglion (O,P). Sites of DiI application are indicated by triangles. Small arrows indicate the vagal (X) motor neurons, which were labeled with DiI that diffused from the application site (P). Single-channel images of the labeled neurons are shown in M′, N′, O′ and P′. These neurons extend dendrites to the contralateral side of the brain. Inset in M′ shows another example in which dendritic processes were clearly labeled. Asterisks indicate r6-derived r7-located neurons, which fail to migrate and remain in r6 in the *llk* embryos. Arrowheads indicate the facial motor nuclei. Dorsal views. Scale bar: 50 μm.

amino acid protein was identified (encompassing exon 16, but no other alternatively used exons; Fig. 5C,D). We refer to this gene product as the wild-type *scrb1* gene in the following experiments. Scrb1 is a cytoplasmic protein carrying a set of 16 leucine-rich repeats (LRR) and four PDZ (for PSD-95/Discs-large/ZO-1) domains (Fig. 5F). Sequence analyses showed that each of the two alleles of the *llk* locus carries a point mutation in the *scrb1* gene. The allele *llk*^{rw16} carries a mis-sense amino acid substitution in the first PDZ domain (I734D), and *llk*^{rw468} carries a stop codon in the LRR domain (K310Stop; Fig. 5E,F).

scrb1 mRNA is expressed in the whole brain

In situ hybridization was performed using the RNA probe that detects all of the spliced variants. The *scrb1* mRNA was expressed maternally during the early embryonic stages. Expression was initially detected throughout the embryo (Fig. 5G-I), but then became restricted to the brain region (Fig. 5J-M). At 18 hpf, when migration of the nVII motor neurons is initiated, *scrb1* mRNA was expressed throughout the neural tube (Fig. 5L,M). However, *scrb1* mRNA was very weakly expressed in the ventral neural tube region, where the

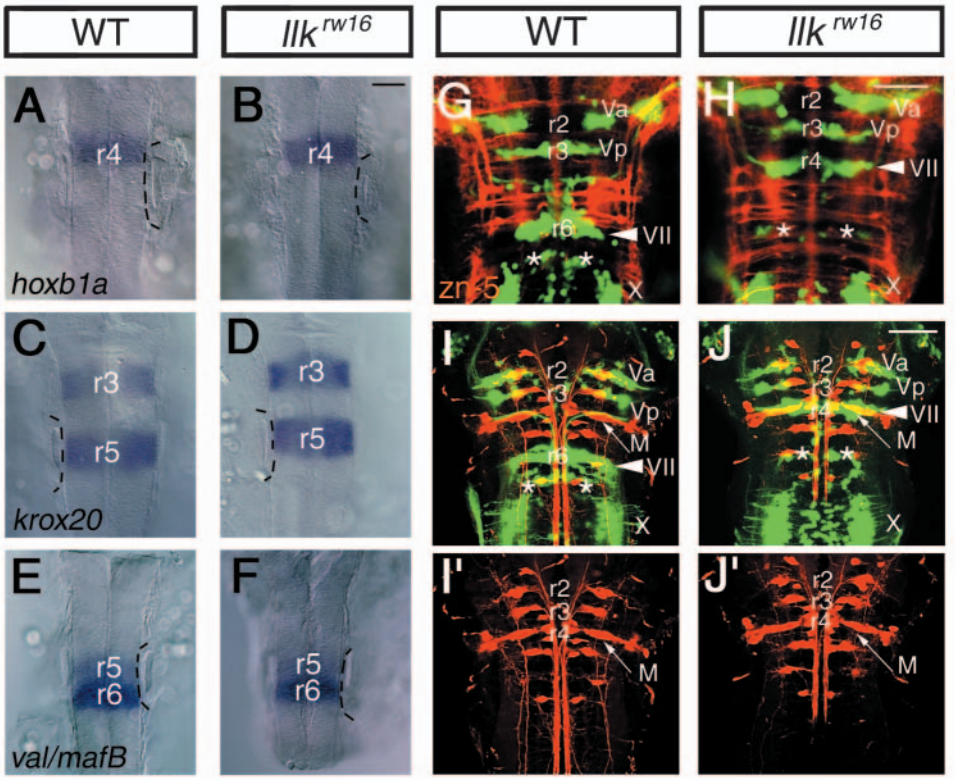

Fig. 4. Rhombomeric patterning and differentiation of the neurons are unaffected in the *llk* embryo. (A,B) *hoxb1a*; (C,D) *krox20*; (E,F) *valentino/mafB* mRNA expression in the wild-type (A,C,E) and *llk*^{rw16} (B,D,F) embryos at 20 hpf. Expression patterns of these genes are unaffected in the *llk*^{rw16} embryo. Dorsal views. The position of the ears are indicated with broken lines. (G,H) Commissural axons are labeled with zn-5 antibody (red) in the wild-type (G) and *llk*^{rw16} (H) embryos at 36 hpf. (I,J) Reticulospinal neurons are retrogradely labeled (red) in the wild-type (I) and *llk*^{rw16} (J) embryos at 5 dpf. Single-channel images of the labeled neurons are shown in separate panels (I′,J′). M, Mauthner's cell. Asterisks indicate r6-derived putative OLe neurons. Arrowheads indicate the facial motor nuclei. Dorsal views. Scale bar: 50 μm.

migrating nVII motor neurons were located (Fig. 5M,M′). Strong expression continued to be observed in the brain during and after the migration of the nVII motor neurons in 22- to 48-hpf embryos (Fig. 5J,K).

Functional knock-down of *scrb1* recapitulates defects of migration of the nVII motor neurons

To confirm that loss of function of the *scrb1* gene is responsible for the *llk* phenotype, antisense morpholino oligos (MO) were designed to specifically disrupt *scrb1* gene function. MO/ATG was designed to abolish translation of *scrb1* maternally and zygotically, while the MO/2e2i abolishes splicing of the gene zygotically. Normal migration of the nVII motor neurons was completely lost in both the resulting morphants compared with the wild-type embryo [5 ng of MO per embryo, Fig. 6B,C, and A, respectively; 100% of MO/ATG-injected embryos (n=82) and 98% of MO/2e2i-injected embryos (n=61)]. Injection of each control MO (MO/ATG-5mis and MO/2e2i-5mis) did not impair migration of nVII motor neurons (0%, n=22 and n=35, respectively), confirming the specificity of the antisense MOs.

Injection of *scrb1* mRNA into one-cell-stage *llk* embryos restores migration of the nVII motor neurons

To confirm the role of the *scrb1* gene in the migration of nVII motor neurons, we generated a wild-type *scrb1* cDNA (Fig. 6D), mutated *scrb1* cDNAs encoding the *llk*^{rw16}, *llk*^{rw468} alleles (*scrb1*^{rw16} and *scrb1*^{rw468}) and a truncated *scrb1* gene encoding only the LRR domain (*scrb1*$^{\Delta PDZs}$) (Fig. 6D). Maternal-and-zygotic (MZ) *llk*^{rw468} embryos were injected with 0.5 ng of each mRNA. MZ-*llk*^{rw468} embryos showed slight CE defects (described in detail below), but these defects were restricted to the tail regions (see below), and the migration phenotype was not affected by the maternal depletion of the gene. When wild-type *scrb1* mRNA was injected into MZ-*llk*^{rw468} homozygous eggs (n=162), 61% of embryos had migration of nVII motor neurons restored (Fig. 6E,F); in 24% this migration was only into r5, and in 37%, migration was fully restored so that neurons moved through r5 into r6. Injection of *scrb1*^{rw16} mRNA (n=175) also rescued the migration phenotype, but only in 10.2% of embryos (5.1% with partial migration to r5, 5.1% with fully restored migration through to r6; Fig. 6G). In contrast, injection of *scrb1*^{rw468} mRNA (n=41) or *scrb1*$^{\Delta PDZs}$ mRNA (n=42) failed to rescue the migration phenotype in any embryos. Thus, both loss-of-function and gain-of-function experiments confirmed that the *llk* locus encompasses the *scrb1* gene.

The *llk* gene acts mainly in a non cell-autonomous manner during migration of the nVII motor neurons

Mosaic experiments were performed to determine the cell autonomy of the *llk* mutation. Wild-type-derived nVII motor neurons failed to migrate caudally in MZ-*llk* host embryos (Fig. 7A). We observed peripheral axons of these cells in each mosaic embryo to ensure that the donor cells were nVII motor neurons. In all of the mosaic embryos examined, a part of the facial motor axons bundle was labeled with rhodamine-dextran (Fig. 7A′), showing that they were indeed nVII motor neurons. These results suggest that the *llk* gene acts in a non cell-autonomous manner during migration of the nVII motor neurons, which is consistent with the observation that *scrb1* mRNA is strongly expressed in the dorsal neural tube cells surrounding the migrating nVII motor neurons (Fig. 5M). In contrast, most of the MZ-*llk*-derived nVII motor neurons migrated normally through r5 into r6 in wild-type host embryos (Fig. 7B). Since some of the late-born neurons remained in r4

at the time of observation, we could not completely exclude the autonomous involvement of the *scrb1* gene in migration of the nVII motor neurons.

Maternal *scrb1* is required for convergent extension movements

Zygotic *llk* embryos do not show any defects in convergent extension (CE) movements and these mutant embryos were homozygously viable (Fig. 2B; 96% of 211 zygotic llk^{rw16} embryos and 97% of 121 zygotic llk^{rw468} embryos survived to larval stages), suggesting that zygotic *llk/scrb1* function is not essential for CE. The *tri/stbm* and *pk1* genes regulate both migration of the nVII motor neurons and CE movements during gastrulation (Jessen et al., 2002; Carreira-Barbosa et al.,

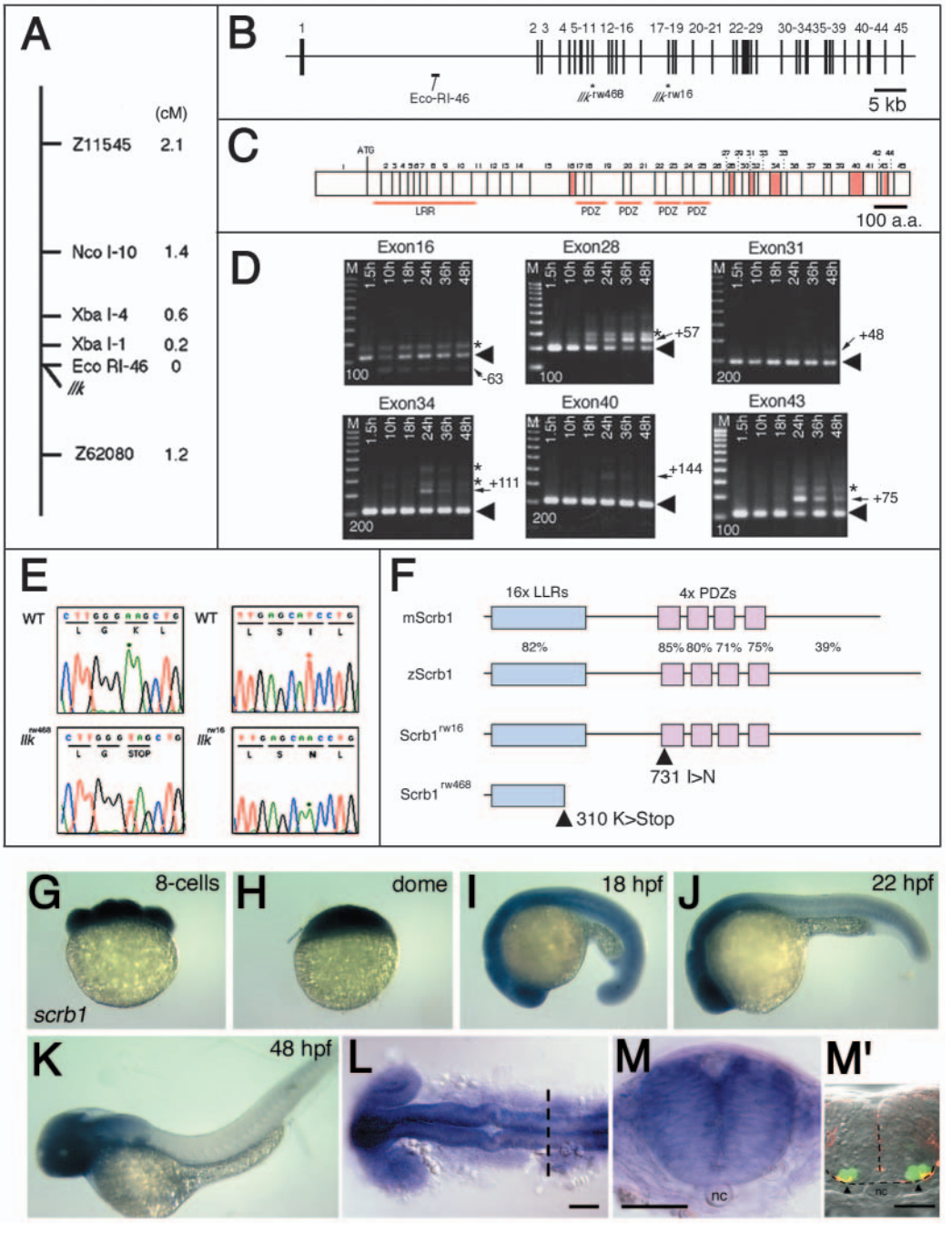

Fig. 5. Identification of the *llk* gene. (A) Genetic map for the *llk* locus. The *llk* locus mapped to linkage group (LG) 7. The RDA marker, EcoRI-46 is located at 0 cM map-distance from the *llk* locus (0 per 2054 meioses). (B) Genomic structure of the zebrafish *scrb1*. The *scrb1* gene is encoded by 45 exons spanning 120 kb in the genome. EcoRI-46 is located in the first intron of the gene. Each of the two mutant alleles, lkl^{rw16} and llk^{rw468}, carries a nucleotide substitution in exons 11 and 17, respectively. (C) Schematic drawing for the putative cDNA encoding 45 exons shown in B. Six alternatively used exons, 16, 28, 31, 34, 40 and 43 are shown as red boxes. Exon numbers and first ATG site are indicated above. Regions encoding LRR domain and four PDZ domains are indicated below. (D) RT-PCR analyses were performed to identify the predominant gene product. Primers were designed in the flanking exons encompassing each exon of interest. Total RNA was extracted from 1.5, 10, 18, 24, 36 and 48-hpf embryos. Arrowheads in each panel indicate the predominant RT-PCR product expressed during migration of the nVII motor neurons at 18-24 hpf. The predominant RT-PCR products contain exon 16, but no other exons (exons 28, 31, 34 and 43). The lesser RT-PCR products contain exons 28, 31, 34 and 43, but not exon 16 (indicated by arrows). 100 bp-interval molecular markers (bp) are shown in each panel. (E) Sequence diagrams of the mutation sites for the llk^{rw16} and llk^{rw468} alleles compared to the wild-type allele. (F) Schematic drawings of the wild-type (zScrb1) and mutant Scrb1 proteins ($Scrb^{rw16}$ and $Scrb^{rw468}$). Percentage identity of the amino acid sequences (%) to the mouse Scrb (mScrb1) is shown for each domain. The allele llk^{rw16} carries a mis-sense amino acid substitution in the first PDZ domain, while llk^{rw468} carries a stop codon in the LRR domain. (G-M) Lateral views of wild-type embryos stained with the *scrb1* RNA probe in the 8-cell stage (G), dome-stage (H), 18 hpf (I), 22 hpf (J) and 48 hpf (K) embryos. (L,M) *scrb1* mRNA expression in the brain at 20 hpf (L, dorsal view) and (M) cross section at r5 (indicated by the broken line in L). M′ shows the cross section at r5 of the 24 hpf-Isl1-GFP embryo stained with anti-acetylated α-tubulin antibody. Arrowheads indicate medial longitudinal fascicles (MLF); nc indicates notochord. Scale bars: 50 μm.

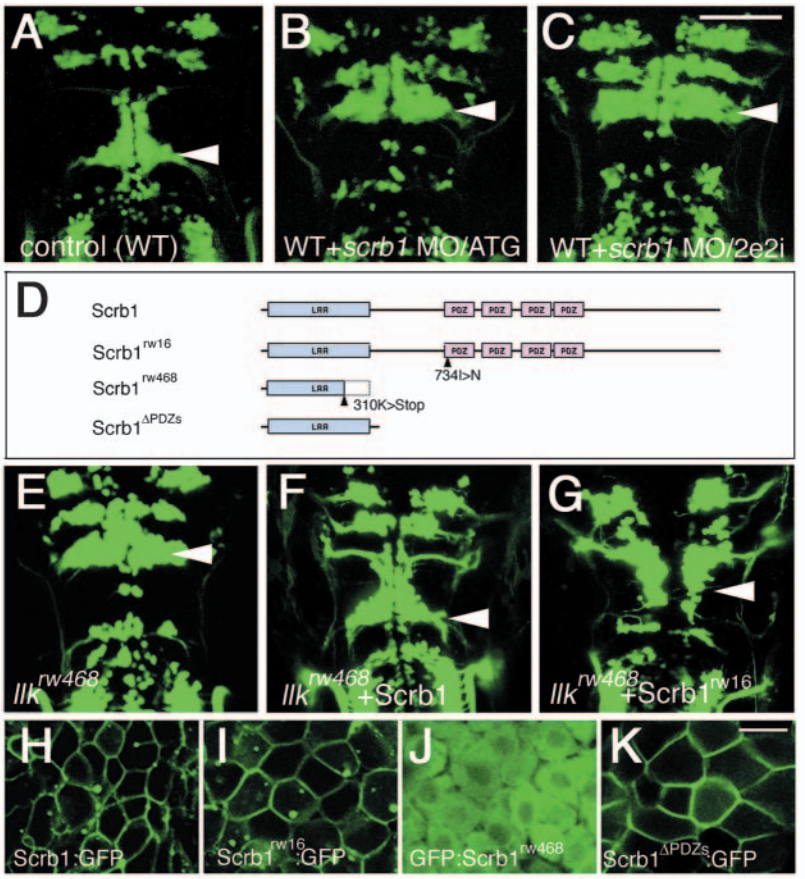

Fig. 6. Loss-of-function and gain-of-function of *scrb1* confirm that *scrb1* is homologous to the *llk* gene. (A-C) Embryos injected with MO did not show any migration of the nVII motor neurons. MOs were designed to disrupt the translation (B, MO/ATG) or splicing (C, MO/2e2i) of the *scrb1* mRNAs (compare with the wild-type embryo shown in A). Dorsal views, 2 dpf. (D-G) Structure-function analyses of Scrb1. Wild-type and mutated *scrb1* mRNAs (schematically drawn in D) were injected into *llk*^{rw468} embryos. Injection of wild-type *scrb1* mRNA restored migration of the nVII motor neurons (F, compare with control *llk*^{rw468} embryo shown in E). Injection of *scrb1*^{rw16} mRNA also restored the migration (G) although at lower frequency. (H-K) Subcellular localization of wild-type and mutated Scrb1 proteins. Scrb1, Scrb1^{rw16} and Scrb1$^{\Delta PDZs}$ are associated with plasma membranes (H,I,K). However, Scrb1^{rw468} failed to localize to membranes (J). A-C, E-G, dorsal views, 2 dpf. H-K, 10-12 hpf. Scale bars: 50 μm (A-G) and 20 μm (H-K).

2003). Since *scrb1* mRNA is strongly expressed maternally (Fig. 5G,H), this gene may also be involved in CE at early stages. Taking advantage of the normal viability of the zygotic *llk* mutants, we were able to generate MZ-*llk* embryos and examine this possibility. Indeed, MZ-*llk* embryos showed slight CE defects during early gastrulation (Fig. 8B,E). They had slightly curled tails in 24-48 hpf (Fig. 8H,J), although some recovered to a normal shape by 4 dpf (4.4% of 113 MZ-*llk*^{rw468} embryos and 53% of 102 MZ-*llk*^{rw16} embryos). To further clarify the role of maternal *scrb1* in CE, *llk*^{rw468} homozygous females were crossed with heterozygous males (+/*llk*^{rw468}). 56% of the resulting embryos (n=123) showed normal nVII motor neuron migration, indicating that they were zygotically heterozygous with no maternal contribution of *scrb1*. The remaining embryos showed loss of the neuron migration, and were MZ-*llk*^{rw468}. Only 28% of the zygotically heterozygous embryos were morphologically normal despite their normal nVII motor neuron migration (n=69). In contrast, 9.3% of the MZ-*llk*^{rw468} embryos were morphologically normal (n=54). These results indicate that maternal *scrb1* is required for CE movements but dispensable for migration of the nVII motor neurons. Moreover, the zygotic *scrb1* expression can compensate for loss of the maternal *scrb1*, but only incompletely. Furthermore, *scrb1* MO/ATG also induced CE defects that were similar to those of MZ-*llk* embryos in all 82 embryos injected (Fig. 8C,F), but injection of *scrb1* MO/2e2i only affected CE in a small proportion

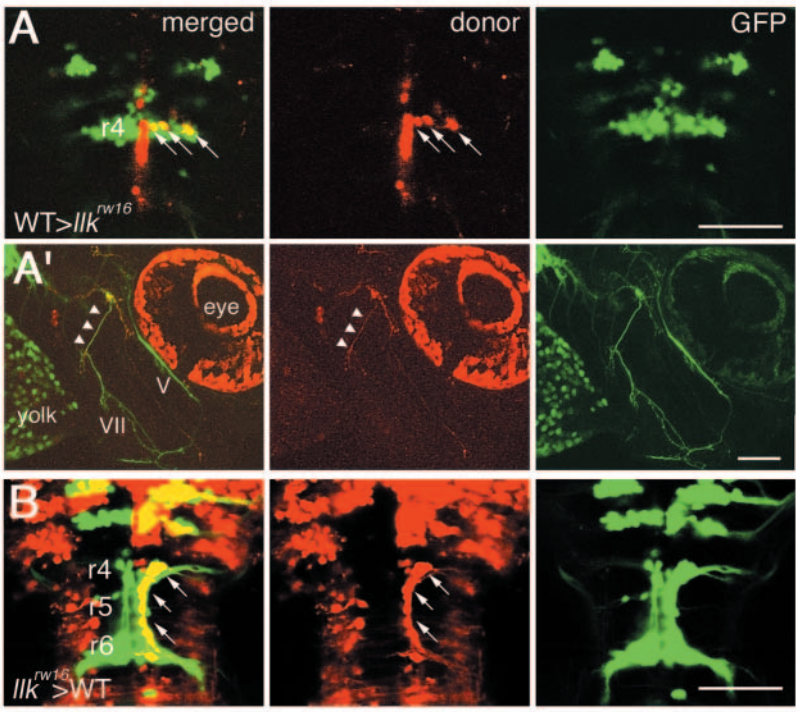

Fig. 7. The *llk* gene is required for migration of the nVII motor neurons in a non cell-autonomous manner. Mosaic experiments were performed to determine the cell autonomy of the *llk* gene. A total of 8 wild-type embryo-derived nVII motor neurons (arrows) all failed to migrate caudally in 3 *llk*^{rw16} host embryos (A). (A′) The peripheral axons (arrowheads) of these cells were comprised in a part of the facial motor axons bundle. (B) In contrast, a total of 21 *llk*^{rw16} embryo-derived nVII motor neurons (arrows) migrated normally through r5 into r6 in 2 wild-type host embryos. (A,B) Dorsal views; (A′) lateral views, anterior is to the right, 2 dpf. Scale bar: 50 μm.

(7.6%, *n*=92) of embryos, confirming that maternal *scrb1* is essential for CE in early development.

Next, we analyzed whether injection of *scrb1* mRNA could rescue CE defects in MZ-*llk*^{rw468} embryos. Injection of 0.5 ng of wild-type *scrb1* mRNA into MZ-*llk*^{rw468} embryos induced recovery of CE defects in 40% of 168 embryos. Injection of 0.5 ng of *scrb1*^{rw16} mRNA into MZ-*llk*^{rw468} embryos also induced recovery of the CE phenotype at a lower frequency (31%, *n*=130). However, injection of 0.5 ng of *scrb1*^{rw468} mRNA (*n*=41) or *scrb1*$^{\Delta PDZs}$ mRNA (*n*=42) failed to rescue the CE phenotype in any embryos. These results indicate that the *scrb1* gene is essential for CE, and that the first PDZ domain of the Scrb1 protein is important for this activity.

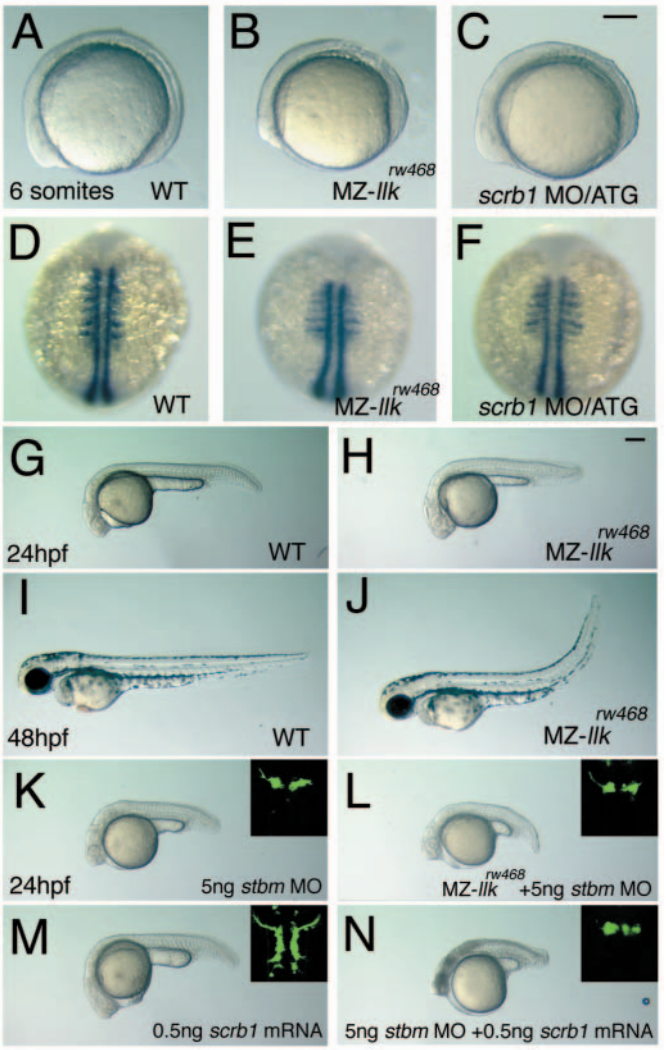

Fig. 8. Maternal *llk/scrb1* is required for convergent extension movements and genetically interacts with *tri/stbm*. (A-F) Maternal and zygotic (MZ-) *llk*^{rw468} embryos show slight convergent extension (CE) defects. Wild-type (A,D), MZ-*llk*^{rw468} (B,E) and *scrb1* MO/ATG-injected (C,F) embryos were observed when alive (A-C) or labeled with *myoD* RNA probe (Weinberg et al., 1996) (D-F). In MZ-*llk*^{rw468} and *scrb1* MO/ATG-injected embryos, the anterior-posterior axis was shorter and somatic mesoderm wider than wild-type embryos. (G-J) Morphology of embryos recovered in the later stages; only tail regions are deficient in MZ-*llk*^{rw468} embryos (H,J; compare with wild-type embryos shown in G,I). (K-N) *llk/scrb1* genetically interacts with *tri/stbm*. (K) Wild-type embryos injected with *stbm* MO show slight CE defects. (L) MZ-*llk*^{rw468} embryos injected with *stbm* MO had slightly greater CE defects. (M) Wild-type embryos injected with *scrb1* mRNA had slight CE defects. (N) Wild-type embryos co-injected with *stbm* MO and *scrb1* mRNA showed severe CE defects. (K-L) Images of the nVII motor neurons in each embryo are shown in insets. Scale bars: 100 μm.

Subcellular localization of Scrb1 and mutated proteins

To analyze the subcellular localization of Scrb1 protein, we injected mRNA from expression vectors encoding wild-type or mutated Scrb1 fused with GFP (Scrb1:GFP) into one-cell stage embryos. Overexpression of the wild-type Scrb1:GFP also rescued the migration of the nVII motor neurons (in 62% of embryos; *n*=45), suggesting that the GFP fusion does not abolish normal function of the original Scrb1. Wild-type Scrb1:GFP protein was localized to the plasma membranes of all cells in which they were overexpressed (5 embryos; Fig. 6H). The mutated Scrb1^{rw16}:GFP and Scrb1$^{\Delta PDZs}$:GFP proteins were both similarly localized to the plasma membrane (5 embryos; Fig. 6I,K). However, mutated Scrb1^{rw468} protein was not associated with the cell membrane, but was localized to the cytoplasm (5 embryos; Fig. 6J). These suggest that the LRR domain is sufficient for the membrane-associated localization of Scrb1 protein. Although Scrb1^{rw16} was localized to the plasma membrane, injection of this construct restored migration of the nVII motor neurons and CE movements in MZ-*llk*^{rw468} embryos only at a lower frequency. Therefore, the membrane-associated localization of Scrb1 by way of the LRR domain is not sufficient, but the first PDZ domain is required for the normal functions of Scrb1.

Genetic interaction between *llk/scrb1* and *tri/stbm*

To determine whether there is an epistatic interaction between the *scrb1* and *stbm* genes in the regulation of migration of the nVII motor neurons, we performed some rescue experiments.

We confirmed that only 0% (*n*=45) and 30% (*n*=37) of embryos injected with 5 ng and 0.5 ng of *stbm* MO, respectively, showed the normal migration of the nVII motor neurons (Fig. 8K). We also confirmed the activity of *stbm* mRNA by using the *tri/stbm* mutant embryos. The *tri*^{rw75} homozygous embryos show the nVII motor neurons migration defects with strong CE defects (Fig. 2D). Sequencing analyses showed that the *tri*^{rw75} allele carries a stop codon (Y342Stop), which results in deletion of the C-terminal intracellular domain of Stbm, and is likely to be a loss-of-function mutation. 22% of embryos obtained from heterozygous *tri*^{rw75} parents show the nVII migration defects as expected (*n*=96). When 0.5 ng of *stbm* mRNA was injected into eggs obtained from heterozygous *tri*^{rw75} parents, only 7.9% of embryos showed the nVII migration defects (*n*=139). These results indicate that 0.5 ng of *stbm* mRNA has activity enough to rescue loss of *stbm* gene function. Similarly, 0.5 ng of *scrb1* mRNA restored the nVII motor neuron migration in MZ-*llk*^{rw468} embryos efficiently as described (Fig. 8F). In contrast, injection of 0.5 ng of *stbm* mRNA into the MZ-*llk*^{rw468} embryos did not restore the migration (0%, *n*=70). Similarly, injection of 0.5 ng of *scrb1* mRNA with 5 ng of *stbm* MO did not restore the neuronal migration (0%, *n*=67). Injection of 0.5 ng of *scrb1* mRNA with 0.5 ng of *stbm* MO also did not restore the neuronal migration (25% of embryos showed the normal

Table 1. Genetic interaction between *scrb1* and *stbm* in the regulation of CE

stbm MO (ng)	*scrb1* mRNA (ng)	CE phenotype*(%)				Number of embryos
		Wild type	*tri*-like	Enhanced	Severe	
0.1	0	97	3	0	0	263
0.1	0.5	83	17	0	0	334
5	0	0	100	0	0	45
5	0.5	0	0	9	91	67

*CE phenotypes were scored at 24 hpf according to the definition in Fig. 8 [wild-type (see Fig. 8G); *tri*-like (see Fig. 8K); enhanced (see Fig. 8L); severe (see Fig. 8N)].

migration, *n*=57). Thus, we conclude that the *scrb1* and *stbm* genes do not act in a simple linear pathway in migration of the nVII motor neurons.

However, we observed strong genetic interactions between *llk/scrb1* and *tri/stbm* genes in CE movements. As previously described (Jessen et al., 2002), injection of 5-50 pg of *stbm* mRNA into wild-type embryos induced CE defects resembling *tri* mutant phenotypes without affecting migration of the nVII motor neurons as judged by the defects in extension of the tail. Overexpression of 0.5 ng of *scrb1* mRNA in wild-type embryos also induced slight CE defects without affecting migration of the nVII motor neurons (63%, *n*=51, Fig. 8M). Injection of 5 ng of *stbm* MO into MZ-*llk*^{rw468} embryos slightly enhanced CE defects (21% of embryos showed enhanced phenotype, *n*=39; Fig. 8L). Injection of 0.5 ng of *stbm* mRNA in the MZ-*llk*^{rw468} embryos significantly enhanced CE defects (14%, *n*=70). More strikingly, co-injection of 5 ng of *stbm* MO together with 0.5 ng of *scrb1* mRNA markedly enhanced CE defects (91% of embryos showed severe defects, *n*=67, Fig. 8N; Table 1). Co-injection of 5 ng of *stbm* MO together with 0.5 ng of *scrb1*^{rw16} mRNA also enhanced CE defects, but at a lower frequency (33% of embryos showed severe defects, *n*=98).

We also carried out additional experiments on genetic interaction between *scrb1* and *stbm* at a suboptimal dose of *stbm* MO. Wild-type embryos were injected with 0.1 ng *stbm* MO and only 3% of resulting embryos showed *tri*-like phenotypes (*n*=263), indicating that this dose is suboptimal. When 0.1 ng of *stbm* MO was injected with 0.5 ng of *scrb1* mRNA, 17% of embryos showed *tri*-like phenotypes (*n*=334). Although the CE defects were not as severe as in embryos injected with 5 ng of *stbm* MO and 0.5 ng of *scrb1* mRNA, the enhancement of CE defects was detected (Table 1).

In conclusion, overexpression of *scrb1* or *stbm* induced the similar CE phenotypes as loss of function of these genes. Moreover, CE was affected most severely when *scrb1* was overexpressed in the absence of *stbm*.

Migration of the nVII motor neurons is not associated with CE movements

It is shown that CE movements of the midline cells are required for neural tube closure in *Xenopus* (Wallingford and Harland, 2002). In mouse embryos, *Crc/Scrb* is required for neural tube closure (Murdoch et al., 2003). Therefore, we wondered if the caudal migration of the nVII motor neurons in normal embryos could be a consequence of any uneven morphogenetic movements of the hindbrain neuroepithelial tissues. For examples, if CE movements proceed more slowly near the ventral midline than in the more lateral region of the r4 tissue, then the medial part including the nVII motor neurons may be left behind by the rest of the r4 tissue and appear to have migrated out from the other r4 tissue. To address this possibility, we labeled the r4 region by uncaging the caged fluorescein-conjugated dextran and traced the cell movements during development (Kozlowski and Weinberg, 2000). We showed that the nVII motor neurons were the only population which came out of the labeled r4 tissue (3 embryos; Fig. 9). These results indicate that the nVII motor neurons migrate completely independently of the rest of the r4 tissues. Thus, we conclude that the uncoordinated CE movements between the tissue surrounding the nVII motor neurons and the rest of the hindbrain is not the cause of the posterior displacement of the nVII motor neurons from r4.

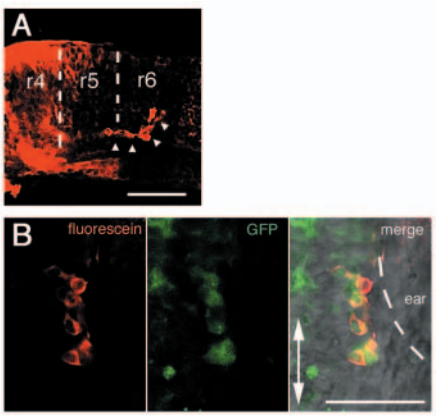

Fig. 9. The nVII motor neurons migrate independently of the rest of the r4 tissues. The r4 region was labeled by uncaging the caged fluorescein-conjugated dextran and the cell movements were traced during development. (A) The nVII motor neurons that migrated into r5 and r6 (arrowheads) were the only population to come out of the labeled r4 tissue. Lateral view, anterior is to the left. (B) Double staining with anti-caged fluorescein and anti-GFP antibodies show that these r4-derived cells are the nVII motor neurons. Ventral views. Scale bars: 50 μm.

Discussion

We have isolated zebrafish mutants with highly specific defects in the caudal migration of the nVII motor neurons, one cause of which is a zygotic defect in *scrb1* function. Taking advantage of the normal viability of the zygotic mutants, we were able to further analyze the role of Scrb1 in early embryogenesis by depletion of maternal transcripts. Our results suggest that *scrb1* plays dual roles in the regulation of cell migration and CE movements, which are differentially controlled by maternal and zygotic expression of *scrb1*, and that *scrb1* interacts with *tri/stbm* gene to regulate CE.

Localization of Scrb1 to the plasma membrane is mediated by the LRR domain

We showed that overexpressed Scrb1 protein is associated with the plasma membrane. Moreover, the LRR domain alone is sufficient for the targeting of this protein to the membrane, which is consistent with previous results (Legouis et al., 2003). *Drosophila* Scribble and the *C. elegans* ortholog LET-413

localize to the basolateral membranes of epithelial cells (Bilder and Perrimon, 2000; Bilder et al., 2000; Legouis et al., 2000). The LRR domain may be required for primary targeting of the protein to the membranes, and then the PDZ domains may be important for precise localization of the protein to specific sites on the membrane, via interaction with other membrane proteins.

Llk/Scrb1 and Tri/Stbm may constitute a functional complex

Recent studies reported that a mammalian homologue *circletail(Crc)/Scrb* is required for neural tube closure and the orientation of sensory cells in the cochlea (Murdoch et al., 2003; Montcouquiol et al., 2003). The defects in the *Crc* embryos are very similar to that in *loop-tail(Lp)* mutants which are the result of mutations in *Van Gogh2*(*Vangl2*)/*stbm*, and *Crc/Scrb* interacts with *Lp/Vangl2/stbm* genetically (Kiber, 2001; Murdoch et al., 2003; Montcouquiol et al., 2003). Thus, in vertebrates, Scrb may act together with Stbm in morphogenesis of neural tissues.

In this study, we showed that injection of *llk/scrb1* mRNA did not rescue migration of the VII motor neurons in *tri/stbm* MO-injected embryos. Similarly, injection of *tri/stbm* mRNA also failed to rescue neuronal migration in the *llk* embryos, suggesting that the *llk/scrb1* and *tri/stbm* genes do not act in a simple linear pathway, but rather that they function by forming a functional complex.

Although our results and previous studies have suggested that there is a genetic interaction between *scrb1* and *stbm* (Murdoch et al., 2003; Montcouquiol et al., 2003), it is not known whether the PDZ domains of Scrb directly interact with the PDZ-binding domain of Stbm. In *Drosophila*, the second PDZ domain of Scrb interacts with Dlg via GUKH (guanylate kinase holder protein) to form a scaffolding complex at synaptic junctions (Mathew et al., 2002). Furthermore, Dlg interacts with Stbm and this complex is required for plasma membrane formation in epithelial cells (Lee et al., 2003). These results suggest that Scrb, Stbm and Dlg may constitute a functional complex during the formation of membrane structures.

If Tri/Stbm and Llk/Scrb1 form a functional complex, this complex would probably have two sites that associate with membranes: the transmembrane domain of Tri/Stbm and the LRR domain of Llk/Scrb1. In this study, we showed that knock-down of Tri/Stbm with overexpression of Llk/Scrb1 led to the most severe impairment of CE. These results indicate that Tri/Stbm may be required for localization of Llk/Scrb1 protein to the specific site of the membrane where they are anchored and function together. Release of membrane-associated Llk/Scrb1 from such positional constraint in the absence of Stbm may have more markedly perturbed the functional protein complexes controlling CE than simple overexpression of Scrb1 in the presence of Stbm.

We also demonstrated that the Scrb1^{rw16} protein, which has a single amino acid substitution in the first PDZ domain, has lower activity than the wild-type protein to rescue migration of the nVII motor neurons in the *llk* mutation. Similarly, overexpression of Scrb1^{rw16} induced CE defects to a lesser extent than that of wild-type Scrb1 protein. These results indicate that the first PDZ domain is also essential for Scrb1 activity. The first PDZ domain of Llk/Scrb1 may interact with another, as yet unidentified, component to establish a multi-protein complex required for its function.

Possible roles of Llk/Scrb1 in migration of the nVII motor neurons

We showed that the *llk/scrb1* gene functions mainly in a non cell-autonomous manner in migration. We also showed that the uncoordinated CE movements between the medial r4 tissue surrounding the nVII motor neurons and the rest of the hindbrain is not likely to be the cause of the posterior displacement of the nVII motor neurons relative to r4. One possibility may be the involvement of the Llk/Scrb1 protein (or the protein complex) in establishing a concentration gradient of attractive cues in the hindbrain. For example, the Llk/Scrb1 protein may interact with a transmembrane protein to capture and display the attractive cues on the surface of cells in the migratory pathway of the nVII motor neurons. Alternatively, the Llk/Scrb1 protein may be required by the neuroepithelial cells to prevent the migrating nVII motor neurons from veering away from the normal migratory pathway as is the case in the *llk* and *ord* embryos (see Fig. 2J,K).

In zebrafish, we showed that several putative OLe neurons are born in r6 and migrate into r7, and that this migration is also impaired in the *llk* embryos. The glossopharyngeal (nIX) motor neurons also failed to migrate from r6 to r7 in the *tri* embryos (Bingham et al., 2002). These results show that there are at least two cell populations that migrate, one from r4 to r6 (nVII motor and r6-located OLe neurons), and the other from r6 to r7 (nIX motor and r7-located putative OLe neurons). The fact that both r4-derived cells and r6-derived cells failed to migrate in the *llk* and *tri* embryos may indicate that the migrations of these cells are regulated by a common mechanism in different rhombomeres. If they are both guided by a common attractive cue emanating from the caudal end of the hindbrain, as was suggested in mouse embryos (Studer, 2001), this cue may have been accumulated to saturation at r6 at which level an effective gradient may have been lost, by the time the r4-derived nVII neurons had arrived at r6.

Similarity and diversity in mechanisms regulating CE and migration of the nVII motor neurons

It has now been shown that *llk/scrb1* (present study), *tri/stbm* (Bingham et al., 2002; Jessen et al., 2002) and *pk1* (Carreira-Barbosa et al., 2003) are required for both CE and neuronal migration. However, the possible PCP signaling molecules *kny/glypican4/6*, *slb/wnt11* and *ppt/wnt5a* regulate CE (Topczewski et al., 2001; Heisenberg et al., 2000; Kilian et al., 2003), but do not regulate neuronal migration (Bingham et al., 2002; Jessen et al., 2002). Moreover, overexpression of a dominant-negative Dishevelled (Dsh), which blocks CE movements (Heisenberg et al., 2000), does not affect the neuronal migration (Jessen et al., 2002). These results suggest that genetic cascades, which regulate the VII motor neuron migration, may not coincide completely with those regulating CE movements.

In this study, we isolated a second mutant, *ord*, in which the nVII motor neurons are misguided away from the normal pathway. Preliminary results showed that the MZ-*ord* embryos did not have any defects in CE movements and are viable. These results suggest that the *ord* gene is only required for neuronal migration, and not for CE. Identification of the gene

responsible for the *ord* mutation may provide us with clues to the mechanisms of neuronal migration, e.g. molecules regulating the attractive guidance cues.

Differentiation and migration of the nVII motor neurons occurs independently

The functions of the nVII motor neurons located ectopically in r4 in morphants or mutants have not been analyzed. In *hoxb1a* knock-down embryos, the non-migratory nVII motor neurons extend peripheral axons normally (McClintock et al., 2002). However, OLe neurons innervating the ear fail to extend axons, indicating that differentiation of these neurons is deficient in these morphants (McClintock et al., 2002). In the *tri* embryos, although all of the non-migratory nVII motor neurons appear to extend axons normally, it is not known whether they are functional because of embryonic lethality (Bingham et al., 2002).

In this study, we were able to address this question, because the *llk* mutation exclusively affects neuronal migration zygotically, and the resultant embryos remain viable. We showed that the nVII motor neurons in the zygotic *llk* embryos failed to migrate and remained at r4, but had normal morphological development. Moreover, the *llk* homozygous larvae showed apparently normal foraging behavior, and the jaw muscles appeared to contract normally. The *llk* homozygous embryos were viable and developed into fertile adults. Therefore, these non-migratory motor neurons must function relatively normally despite their aberrant localization. Since many genes have been implicated in migration of the VII motor neurons and this process has been conserved in evolution (Studer et al., 1996; Garel et al., 2000; Ohshima et al., 2002; Muller et al., 2003), it is unlikely that correct migration of nVll motor neurons has been maintained without any survival advantage. Thus, it is rather more likely that mislocation of the nVII motor neurons in the *llk* embryos may be epigenetically compensated for by reorganization of neural networks during development. This innate developmental plasticity may have laid the basis for accommodating the loss of migration of the nVII motor neurons during evolution to avian species (Studer, 2001).

Possible functional redundancy within LAP family genes

In *Drosophila scribble* and *C. elegans let-413* mutants, cell-cell junctions are not positioned properly, resulting in embryonic death with severe apicobasal polarity defects in epithelial cells (Bilder and Perrimon, 2000; Bilder et al., 2000; Legouis et al., 2000). However, in mice (Murdoch et al., 2003; Montcouquiol et al., 2003) and in zebrafish (this study), *scrb1* mutant embryos appear to have normal epithelial cells. Four LAP family genes (*scribble1*, *erbin*, *densin-180* and *lano*) have been identified in mice (reviewed by Santoni et al., 2002). Therefore, it is possible that other LAP family genes may have overlapping or redundant functions in epithelial formation in vertebrate species. In zebrafish, at least four LAP family genes were also identified in the genome database (corresponding to *llk/scribble1*, *erbin*, *densin-180* and *lano*, data not shown). Putative zebrafish *erbin* and *lano* mRNA was strongly expressed maternally (data not shown), thus these genes are good candidates to compensate for loss of Scribble1 function in epithelial polarity formation in vertebrates.

In *Crc/Scrb* mutant mice embryos neural tube closure is severely deficient (Murdoch et al., 2003). In contrast, there is no neural tube defect in zygotic or MZ-*llk* embryos in zebrafish. It is possible that unidentified zebrafish *scribble1* homologs may regulate neurulation independently of *llk/scrb1* function. Alternatively, neurulation in zebrafish may be achieved by mechanisms different from that in mice (reviewed by Lowery and Sive, 2004). In mice, a neural tube with an open ventricle lumen forms by folding of the neural plate epithelium. In contrast, in zebrafish, the neural plate forms a solid neural keel, then a lumen opens in its midline to form the tube (reviewed by Lowery and Sive, 2004). Thus, it is possible that *llk/scrb1* function may not be required for the teleost-specific neurulation steps.

We thank J. Kuwada, T. Jowett, and C. Moens for gifts of cDNA clones; A. Shimada for assistance; A. Thomson for critical reading of the manuscript. This research was supported in part by Grant-in-Aid and Special Coordination Fund from the Ministry of Education, Science, Technology, Sports and Culture of Japan, and grants for Core Research for Evolutional Science and Technology from the Japan Science and Technology Corporation (JST).

Supplementary material

Supplementary material for this article is available at
http://dev.biologists.org/cgi/content/full/132/10/2273/DC1

References

Ando, H. and Okamoto, H. (2003). Practical procedures for ectopic induction of gene expression in zebrafish embryos using Bhc-diazo-caged mRNA. *Methods Cell Sci.* **25**, 25-31.

Ando, H., Furuta, T., Tsien, R. Y. and Okamoto, H. (2001). Photo-mediated gene activation using caged RNA/DNA in zebrafish embryos. *Nat. Genet.* **28**, 317-325.

Bilder, D. and Perrimon, N. (2000). Localization of apical epithelial determinants by the basolateral PDZ protein Scribble. *Nature* **403**, 676-680.

Bilder, D., Li, M. and Perrimon, N. (2000). Cooperative regulation of cell polarity and growth by *Drosophila* tumor suppressors. *Science* **289**, 113-116.

Bingham, S., Higashijima, S., Okamoto, H. and Chandrasekhar, A. (2002). The Zebrafish *trilobite* gene is essential for tangential migration of branchiomotor neurons. *Dev. Biol.* **242**, 149-160.

Carreira-Barbosa, F., Concha, M. L., Takeuchi, M., Ueno, N., Wilson, S. W. and Tada, M. (2003). Prickle 1 regulates cell movements during gastrulation and neuronal migration in zebrafish. *Development* **130**, 4037-4046.

Chandrasekhar, A., Moens, C. B., Warren J. T., Jr, Kimmel, C. B. and Kuwada, J. Y. (1997). Development of branchiomotor neurons in zebrafish. *Development* **124**, 2633-2644.

Garel, S., Garcia-Dominguez, M. and Charnay, P. (2000). Control of the migratory pathway of facial branchiomotor neurones. *Development* **127**, 5297-5307.

Heisenberg, C. P., Tada, M., Rauch, G. J., Saude, L., Concha, M. L., Geisler, R., Stemple, D. L., Smith, J. C. and Wilson, S. W. (2000). Silberblick/Wnt11 mediates convergent extension movements during zebrafish gastrulation. *Nature* **405**, 76-81.

Higashijima, S., Hotta, Y. and Okamoto, H. (2000). Visualization of cranial motor neurons in live transgenic zebrafish expressing green fluorescent protein under the control of the islet-1 promoter/enhancer. *J. Neurosci.* **20**, 206-218.

Jessen, J. R., Topczewski, J., Bingham, S., Sepich, D. S., Marlow, F., Chandrasekhar, A. and Solnica-Krezel, L. (2002). Zebrafish *trilobite* identifies new roles for Strabismus in gastrulation and neuronal movements. *Nat. Cell Biol.* **4**, 610-615.

Kibar, Z., Vogan, K. J., Groulx, N., Justice, M. J., Underhill, D. A. and Gros, P. (2001). Ltap, a mammalian homolog of *Drosophila* Strabismus/Van Gogh, is altered in the mouse neural tube mutant Loop-tail. *Nat. Genet.* **28**, 251-255.

Kilian, B., Mansukoski, H., Barbosa, F. C., Ulrich, F. and Tada, M. and

Heisenberg, C. P. (2003). The role of Ppt/Wnt5 in regulating cell shape and movement during zebrafish gastrulation. *Mech. Dev.* **120**, 467-476.
Kozlowski, D. J. and Weinberg, E. S. (2000). Photoactivatable (caged) fluorescein as a cell tracer for fate mapping in the zebrafish embryo. *Methods Mol. Biol.* **135**, 349-355.
Lee, O. K., Frese, K. K., James, J. S., Chadda, D., Chen, Z. H., Javier, R. T. and Cho, K. O. (2003). Discs-Large and Strabismus are functionally linked to plasma membrane formation. *Nat. Cell Biol.* **5**, 987-993.
Legouis, R., Gansmuller, A., Sookhareea, S., Bosher, J. M., Baillie, D. L. and Labouesse, M. (2000). LET-413 is a basolateral protein required for the assembly of adherens junctions in *Caenorhabditis elegans*. *Nat. Cell Biol.* **2**, 415-422.
Legouis, R., Jaulin-Bastard, F., Schott, S., Navarro, C., Borg, J. P. and Labouesse, M. (2003). Basolateral targeting by leucine-rich repeat domains in epithelial cells. *EMBO Rep.* **4**, 1096-1102.
Lisitsyn, N., Lisitsyn, N. and Wigler, M. (1993). Cloning the differences between two complex genomes. *Science* **259**, 946-951.
Masai, I., Lele, Z., Yamaguchi, M., Komori, A., Nakata, A., Nishiwaki, Y., Wada, H., Tanaka, H., Nojima, Y., Hammerschmidt, M. et al. (2003). N-cadherin mediates retinal lamination, maintenance of forebrain compartments and patterning of retinal neurites. *Development* **130**, 2479-2494.
Matsuda, N. and Mishina, M. (2004). Identification of chaperonin CCT gamma subunit as a determinant of retinotectal development by whole-genome subtraction cloning from zebrafish no tectal neuron mutant. *Development* **131**, 1913-1925.
Mathew, D., Gramates, L. S., Packard, M., Thomas, U., Bilder, D., Perrimon, N., Gorczyca, M. and Budnik, V. (2002). Recruitment of scribble to the synaptic scaffolding complex requires GUK-holder, a novel DLG binding protein. *Curr. Biol.* **12**, 531-539.
McClintock, J. M., Kheirbek, M. A. and Prince, V. E. (2002). Knockdown of duplicated zebrafish *hoxb1* genes reveals distinct roles in hindbrain patterning and a novel mechanism of duplicate gene retention. *Development* **129**, 2339-2354.
Metcalfe, W. K., Mendelson, B. and Kimmel, C. B. (1986). Segmental homologies among reticulospinal neurons in the hindbrain of the zebrafish larva. *J. Comp. Neurol.* **251**, 147-159.
Moens, C. B., Yan, Y. L., Appel, B., Force, A. G. and Kimmel, C. B. (1996). valentino: a zebrafish gene required for normal hindbrain segmentation. *Development* **122**, 3981-3990.
Moens, C. B., Cordes, S. P., Giorgianni, M. W., Barsh, G. S. and Kimmel, C. B. (1998). Equivalence in the genetic control of hindbrain segmentation in fish and mouse. *Development* **125**, 381-391.
Montcouquiol, M., Rachel, R. A., Lanford, P. J., Copeland, N. G., Jenkins, N. A. and Kelley, M. W. (2003). Identification of Vangl2 and Scrb1 as planar polarity genes in mammals. *Nature* **423**, 173-177.
Muller, M., Jabs, N., Lork, D. E., Fritzsch, B. and Sander, M. (2003). Nkx6.1 controls migration and axon pathfinding of cranial branchio-motoneurons. *Development* **130**, 5818-5826.
Murdoch, J. N., Henderson, D. J., Doudney, K., Gaston-Massuet, C., Phillips, H. M., Paternotte, C., Arkell, R., Stanier, P. and Copp, A. J. (2003). Disruption of *scribble* (Scrb1) causes severe neural tube defects in the circletail mouse. *Hum. Mol. Genet.* **12**, 87-98.
Nasevicius, A. and Ekker, S. C. (2000). Effective targeted gene 'knockdown' in zebrafish. *Nat. Genet.* **26**, 216-220.
Ohshima, T., Ogawa, M., Takeuchi, K., Takahashi, S., Kulkarni, A. B. and Mikoshiba, K. (2002). Cyclin-dependent kinase 5/p35 contributes synergistically with Reelin/Dab1 to the positioning of facial branchiomotor and inferior olive neurons in the developing mouse hindbrain. *J. Neurosci.* **22**, 4036-4044.
Oxtoby, E. and Jowett, T. (1993). Cloning of the zebrafish krox-20 gene (krx-20) and its expression during hindbrain development. *Nucleic Acids Res.* **21**, 1087-1095.
Prince, V. E., Moens, C. B., Kimmel, C. B. and Ho, R. K. (1998). Zebrafish hox genes: expression in the hindbrain region of wild-type and mutants of the segmentation gene, valentino. *Development* **125**, 393-406.
Sato, T. and Mishina, M. (2003). Representational difference analysis, high-resolution physical mapping, and transcript identification of the zebrafish genomic region for a motor behavior. *Genomics* **82**, 218-229.
Solnica-Krezel, L., Schier, A. F. and Driever, W. (1994). Efficient recovery of ENU-induced mutations from the zebrafish germline. *Genetics* **136**, 1401-1420.
Shimoda, N., Knapik, E. W., Ziniti, J., Sim, C., Yamada, E., Kaplan, S., Jackson, D., de Sauvage, F., Jacob, H. and Fishman, M. C. (1999). Zebrafish genetic map with 2000 microsatellite markers. *Genomics* **58**, 219-232.
Strutt, D. (2003). Frizzled signalling and cell polarisation in *Drosophila* and vertebrates. *Development* **130**, 4501-4513.
Studer, M., Lumsden, A., Ariza-McNaughton, L., Bradley, A. and Krumlauf, R. (1996). Altered segmental identity and abnormal migration of motor neurons in mice lacking Hoxb-1. *Nature* **386**, 630-634.
Studer, M. (2001). Initiation of facial motoneurone migration is dependent on rhombomeres 5 and 6. *Development* **128**, 3707-3716.
Topczewski, J., Sepich, D. S., Myers, D. C., Walker, C., Amores, A., Lele, Z., Hammerschmidt, M., Postlethwait, J. and Solnica-Krezel, L. (2001). The zebrafish glypican *knypek* controls cell polarity during gastrulation movements of convergent extension. *Dev. Cell* **1**, 251-264.
Trevarrow, B., Marks, D. L. and Kimmel, C. B. (1990). Organization of hindbrain segments in the zebrafish embryo. *Neuron* **4**, 669-679.
Wallingford, J. B. and Harland, R. M. (2002). Neural tube closure requires Dishvelled-dependent convergent extension of the midline. *Development* **129**, 5815-5825.
Warren, J. T. Jr, Chandrasekhar, A., Kanki, J. P., Rangarajan, R., Furley, A. J. and Kuwada, J. Y. (1999). Molecular cloning and developmental expression of a zebrafish axonal glycoprotein similar to TAG-1. *Mech. Dev.* **80**, 197-201.
Westerfield, M. (1995). *The Zebrafish Book*. Eugene, Oregon: University of Oregon.
Weinberg, E. S., Allende, M. L., Kelly, C. S., Abdelhamid, A., Murakami, T., Andermann, P., Doerre, O. G., Grunwald, D. J. and Riggleman, B. (1996). Developmental regulation of zebrafish MyoD in wild-type, no tail and spadetail embryos. *Development* **122**, 271-280.